

# Fluid Mass Associated with an Axisymmetric Parachute Canopy

Paul C. Klimas\*

Sandia Laboratories, Albuquerque, N. M.

An analytical technique for calculating the fluid mass associated with parachute canopies of arbitrary axisymmetric cross section operating in an inviscid, incompressible fluid is presented. The effects of porosity, both nominal and geometric, are included. The procedure replaces the physical parachute canopy with a mathematical vortex sheet of a strength which is determined through application of velocity boundary conditions. The strength then is used to find the fluid kinetic energy. Equating this energy to the system translational kinetic energy gives the mass in question. Final and intermediate results compare favorably with those of previous analysis and experiment.

## I. Introduction

**K**NOWLEDGE of the air mass associated with the trajectory of a parachute canopy is required to describe that trajectory analytically. Because of the complexities associated with typical canopy geometries and the porous nature of their surfaces, computations in the past have relied very heavily upon experimental determination of this mass. This paper details a procedure for calculating the sum of included and additional mass inherent in the axial motion of parachutes with arbitrary axisymmetric cross sections.

## II. Analysis

Lamb<sup>1</sup> gives the kinetic energy of a stream of vortex rings immersed in an incompressible, inviscid fluid which is at rest at infinity as

$$T = \pi \rho \sum \Gamma \Psi \quad (1)$$

where

$T$  = kinetic energy

$\rho$  = fluid density

$\Gamma$  = strength of an individual vortex ring

$\Psi$  = value of the stream function at the vortex ring under consideration

and where the summation is taken over all of the rings in the system. Equation (1) may be modified to apply to a system of axisymmetric vortex sheets through

$$T = \pi \rho \int \gamma \psi ds \quad (2)$$

where  $\gamma \equiv d\Gamma/ds$  and  $s$  is the coordinate measured along the sheet or sheets comprising the system. Since  $T = \frac{1}{2} m V^2$ , where  $V$  is the known speed of the system and  $m$  the sought-after mass of fluid set in motion by the vortex sheets, a vortex sheet parachute aerodynamic model in which  $\gamma$  and  $\Psi$  were known would allow equating the two kinetic energy expressions and subsequent solution for  $m$ .

Modeling a parachute canopy by a vortex sheet placed to coincide with the physical location of the canopy (Fig. 1) is quite appropriate. This type of singularity has zero thickness,

thus resembling a thin fabric, and porosity may be built in by constructing gaps in individual sheets representing the canopy or otherwise allowing flow across the sheets.

The approach taken here will be to obtain the sheet strength distribution by applying velocity boundary conditions. Once these  $\gamma$ 's have been found, they will be used to compute the required stream function values. For computational convenience, the sheet takes the form of conical frustum segments which run between preselected points along the actual canopy boundary (Fig. 2). Along each segment the vortex sheet strength  $\gamma$  is allowed to vary linearly between "corner" points. Here, arbitrarily choosing the segment between corners 1 and 2, the local sheet strength is

$$\gamma = [(\gamma_2 - \gamma_1) / (s_2 - s_1)] (s - s_1) + \gamma_1$$

where  $s$  is the location coordinate measured along the sheet from its beginning in space and the subscripts denote corner values. The axial and radial velocity components at a point  $(x, r)$  in space due to a segment of sheet between  $s_1$  and  $s_2$  may be written from the Biot-Savart Law as

$$\begin{aligned} u &= \frac{(\gamma_2 - \gamma_1)}{2\pi(s_2 - s_1)} \int_{s_1}^{s_2} \frac{s}{r_1} \left\{ K - E \left[ 1 + \frac{2r'(r-r')}{r_2^2} \right] \right\} ds \\ &\quad - \frac{(\gamma_2 s_1 - \gamma_1 s_2)}{2\pi(s_2 - s_1)} \int_{s_1}^{s_2} \frac{1}{r_1} \left\{ K - E \left[ 1 + \frac{2r'(r-r')}{r_2^2} \right] \right\} ds \\ v &= \frac{(\gamma_1 - \gamma_2)}{2\pi r(s_2 - s_1)} \int_{s_1}^{s_2} \frac{(x-x')s}{r_1} \left\{ K - E \left[ 1 + \frac{2rr'}{r_2^2} \right] \right\} ds \\ &\quad + \frac{(\gamma_2 s_1 - \gamma_1 s_2)}{2\pi r(s_2 - s_1)} \int_{s_1}^{s_2} \frac{(x-x')}{r_1} \left\{ K - E \left[ 1 + \frac{2rr'}{r_2^2} \right] \right\} ds \end{aligned}$$

in which

$$r_1^2 = (x-x')^2 + (r+r')^2$$

$$r_2^2 = (x-x')^2 + (r-r')^2$$

and where  $K$  and  $E$  are complete elliptic integrals and are defined along with their modulus  $k$  by the following:

$$K = \int_0^{\pi/2} \frac{d\alpha}{[1 - k^2 \sin^2 \alpha]^{1/2}}$$

$$E = \int_0^{\pi/2} [1 - k^2 \sin^2 \alpha]^{1/2} d\alpha$$

$$k^2 = 4rr' / r_1^2$$

Presented as Paper 75-1352 at the AIAA 5th Aerodynamic Deceleration Systems Conference, Albuquerque, N. Mex., Nov. 17-19, 1975; submitted Jan. 15, 1976; revision received Feb. 24, 1977.

Index categories: Aerodynamics; Deceleration Systems.

\*Member of Technical Staff, Aerodynamics Department 1330. Member AIAA.

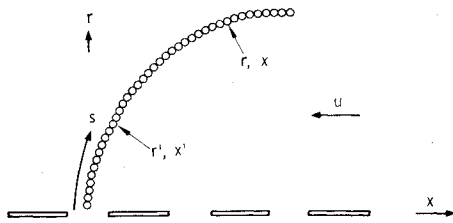


Fig. 1 Parachute replaced by a vortex sheet composed of ring vortices.

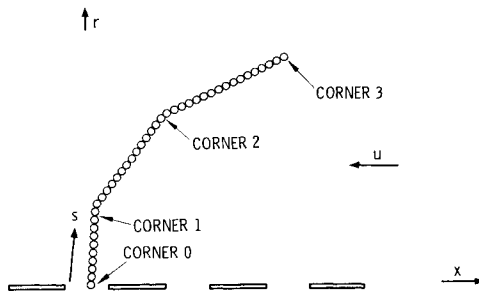


Fig. 2 Canopy sheet of Fig. 1 replaced by conical frustum sheet segments for computational convenience.

with the angle  $\alpha$  being the circumferential location of a point around the frustum, and  $x'$ ,  $r'$  the axial and radial locations of a point on the frustum, respectively. Note that these equations may be integrated without knowledge of the specific values of the  $\gamma_1$  or  $\gamma_2$ .

In the case of continuous surface canopies the number of unknown  $\gamma$ 's is equal to the number of conical frustum segments ( $N$ ) plus one. All but one of these unknowns are found by requiring that the velocity contributions of each segment plus that of the freestream be tangent to the sheet at some point on each frustum. Specification of the last unknown is made a priori by requiring the fluid to leave the trailing edge of the sheet smoothly (the Kutta condition employed in airfoil analyses). Then one of the  $\gamma$ 's is zero and the velocity equations yield a set of  $N$  simultaneous linear algebraic equations in the remaining  $N$  unknown  $\gamma$ 's. Discrete application of the no-normal-flow boundary condition does not present a drawback. With this procedure there is flow across the canopy surface between the boundary condition points, thus modeling a porous fabric. For ribbon parachutes (or other discontinuous surface types), the number of unknown  $\gamma$ 's is equal to the number of frustum segments plus the number of ribbons (or the number of physical surfaces) comprising the canopy. Again, the velocity boundary conditions provide enough equations for the first group and a Kutta condition application at the trailing edge of each ribbon or surface will send the remainder to zero. Note that the form of velocity boundary conditions used here implies steady-state operation. However, there is no obstacle to including a dynamic boundary.

Once the  $\gamma$ 's are available, the other required quantity in Eq. (2) may be obtained. The stream function<sup>2</sup> associated with one such segment is

$$\Psi = \frac{\gamma_2 - \gamma_1}{2\pi(s_2 - s_1)} \int_{s_1}^{s_2} \left\{ \left[ \frac{(x - x')^2 + r^2 + r'^2}{r_1} \right] K - r_1 E \right\} ds$$

$$- \frac{(\gamma_2 s_1 - \gamma_1 s_2)}{2\pi(s_2 - s_1)} \int_{s_1}^{s_2} \left\{ \left[ \frac{(x - x')^2 + r^2 + r'^2}{r_1} \right] K - r_1 E \right\} ds$$

### III. Numerical Calculation

As long as the point at which the velocity is sought does not lie on the contributing portion of the sheet, integration of the

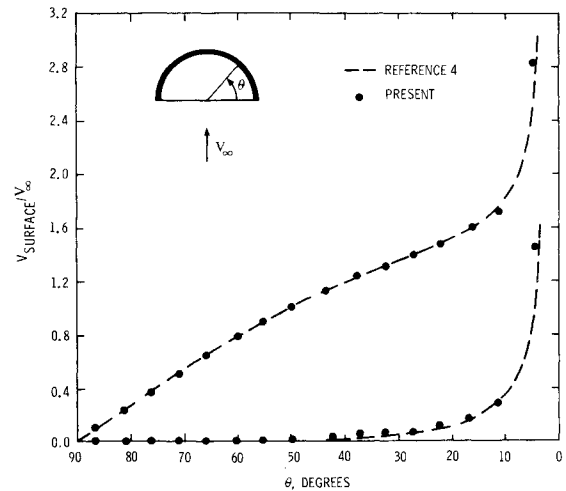


Fig. 3 Velocity distribution on hemispherical cup.

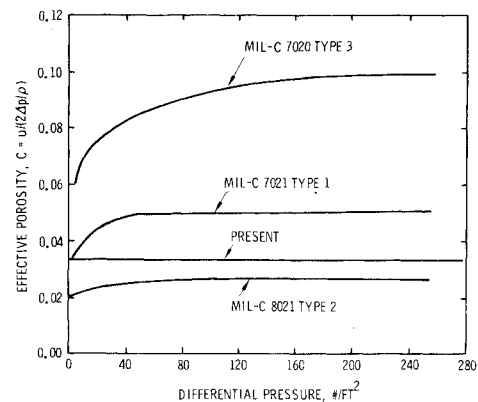


Fig. 4 The effective porosity of parachute materials vs differential pressure.

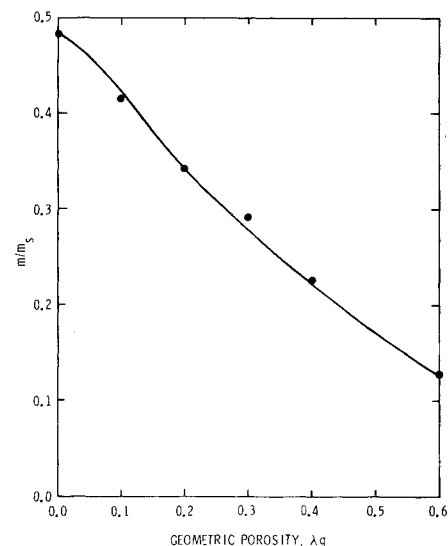


Fig. 5 Fluid mass ratios of hemispherical cup ribbon parachutes.

velocity equations is straightforward. The elliptic integrals,  $K$  and  $E$ , here were evaluated using standard computer subroutines. The  $s$ -type integrals were evaluated using 4-10-point Gaussian quadrature routines,<sup>3</sup> depending upon the proximity of the contributing frustum to the point where the velocity was being evaluated. If, however, the latter point fell on the contributing segment, the integral became improper. In these cases a characteristic peculiar to vortex sheets was used

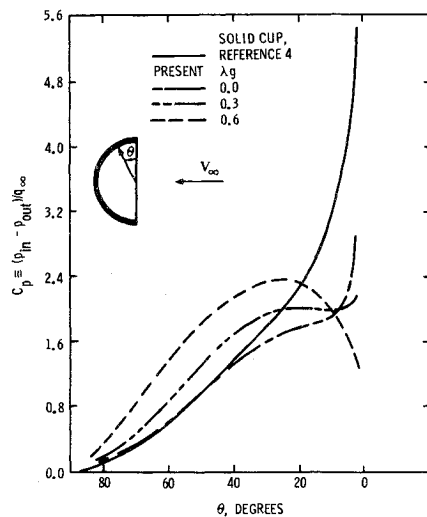


Fig. 6 Differential surface pressures on hemispherical cup parachutes.

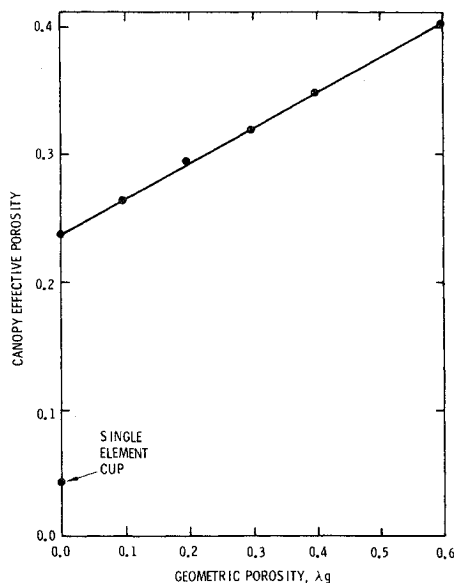


Fig. 7 Canopy effective porosity of hemispherical cup ribbons.

to evaluate the integrals in question. The velocity of a point on a vortex sheet is not a function of the infinitesimal sheet area upon which it is located. Consequently, it was felt that the velocity contribution could be evaluated adequately by integrating from the beginning of the segment to within a very small distance of the boundary condition point, stopping, and then resuming the integration from a very small distance beyond the point to the end of the segment. Trial and error showed that essential convergence was attained by omitting the interval between  $\pm 0.0001 (s_2 - s_1)$  of the boundary condition point. The  $N$  simultaneous linear equations in the  $N$  unknown  $\gamma$ 's expressing the no-normal-flow boundary condition then were solved by matrix inversion subroutines to produce the  $\gamma$ 's.

#### IV. Results

The validity of the vortex sheet representation may be assessed by modeling a solid hemispherical cup and comparing the surface velocity distributions with those calculated analytically by Ibrahim.<sup>4</sup> This (steady-state) comparison is given in Fig. 3. The model assumed 16 equal surface length frustums, and the no-normal flow boundary conditions were applied at the midpoint of each segment. The porosity of mathematical "fabric" was negligible for all elements except

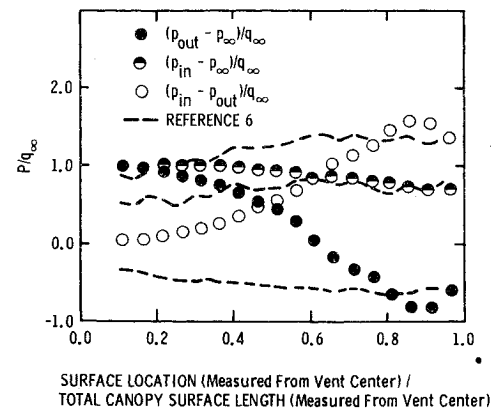


Fig. 8 Surface pressures on a fully inflated 10% geometric porosity ribbon parachute.

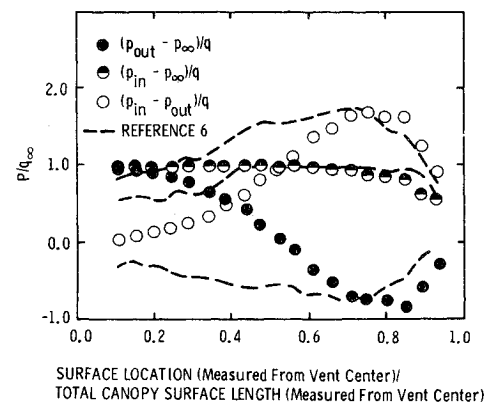


Fig. 9 Surface pressures on a fully inflated 25% geometric porosity ribbon parachute.

for that one which was nearest the skirt. Because fluid speeds become infinite at vortex sheet edges having nonzero strengths, there exist very high pressure differentials near these edges and correspondingly high mass flows across the sheets. The effective porosity of the canopy (defined as the ratio of average velocity normal to the fabric to the freestream velocity) was 0.044. This value is shown in Fig. 4 along with some actual fabric data.<sup>5</sup> The result of equating Eq. (2) to  $\frac{1}{2} m V^2$  for this canopy gave an associated fluid mass of  $0.9938 m_s$ , where  $m_s$  is the mass of fluid displaced by a sphere having a radius equal to that of the cup. This compares to Ibrahim's value of  $1.068 m_s$ , the lower present value being attributable to leakage across the canopy surface.

The trend of decreasing associated fluid mass with increasing porosity is seen in the Fig. 5 plot of  $m/m_s$  for hemispherical ribbon parachutes of varying geometric porosity ( $\lambda_g$ ). The model assumed 16 equal surface-length ribbons whose vortex sheet strengths varied from zero at each ribbon trailing edge linearly to the leading edge value which caused the no-normal-flow boundary condition to be satisfied at the midpoint of each ribbon. The validity of this representation may be judged from the Fig. 6 plot of differential surface pressures. The  $\lambda_g = 0$  version does not coincide with the solid surface result, this being because of appreciable fabric porosity. This porosity is directly attributable to the discontinuous distribution of sheet strength, there now being 16 nonzero strength sheet edges. The effective porosity was  $0.232 \pm 0.007$  for all values of  $\lambda_g$  considered. Relative to the solid cup, the lower pressures near the skirt of the porous models arise from a lower degree of turning required of the fluid here whereas the opposite is the case farther back on the surface. The effective porosities of the entire canopies (ribbons plus gaps) are shown in Fig. 7.

Some actual ribbon canopies also have been modeled. The experimental<sup>6</sup> and calculated pressure distributions on two

fully inflated, steadily operating 10 and 25%  $\lambda g$  ribbon parachutes are given in Figs. 8 and 9, respectively. The pressures agree reasonably well over the portions of the canopies which are forward of the probable separation points. The better overall agreement seen in the 25%  $\lambda g$  case is likely due in part to the easier replacement of low-energy outer-surface air by high-energy internal air through the relatively wide ribbon gaps. In this way the actual flow near the surface more closely resembles that of an inviscid fluid. The boundary condition application points were 20 and 28% of ribbon width measured from the ribbon trailing edges for the  $\lambda g = 0.10$  and  $\lambda g = 0.25$  cases, respectively. Moving these points aft from the mid-element location has the effect of reducing differential pressures, and, consequently, the mass flow across the sheet. The "fabric" effective porosities were 0.061 for the  $\lambda g = 0.010$  model and 0.122 for the 0.25 version. The qualitative behavior continued into the canopy effective porosities, which were 0.127 and 0.256. The  $m/m_s$  value for the 10% canopy was 0.749, whereas that for the higher porosity example was expectedly lower at  $m/m_s = 0.414$ . Here  $m_s$  was based on a sphere whose radius equaled the maximum radial dimension of the inflated canopy.

### V. Conclusions

The ability to calculate fluid masses associated with parachute canopies of fixed arbitrary axisymmetric cross

section operating in an incompressible, inviscid fluid has been demonstrated. No obstacle exists to extension of the approach to include nonsteady geometries.

### Acknowledgment

This work was supported by the U. S. Energy Research and Development Administration.

### References

- <sup>1</sup>Lamb, H., *Hydrodynamics*, 6th ed., Dover Publications, New York, 1945, p. 239.
- <sup>2</sup>Sadowsky, M. A. and Sternberg, E., "Elliptic Integral Representation of Axially Symmetric Flows," *Quarterly of Applied Mathematics*, Vol. VIII, July 1950, pp. 113-126.
- <sup>3</sup>Trulin, D. V., "A Method for Computing the Pressure Distribution about an Axisymmetric Nacelle in Subsonic Flow," Ph.D. Thesis, Iowa State University, Ames, Iowa, 1968.
- <sup>4</sup>Ibrahim, S. K., "Apparent Added Mass and Moment of Inertia of Cup-Shaped Bodies in Unsteady Incompressible Flow," Ph.D. Thesis, University of Minnesota, May 1965.
- <sup>5</sup>Heinrich, H. G., "The Effective Porosity of Parachute Cloth," *Short Course in Aerodynamic Deceleration*, University of Minnesota, 1969.
- <sup>6</sup>Holbrook, J. W., "Sandia Corporation Pressure and Disreefing Test of Model Parachutes in The Vought System Division Low Speed Wind Tunnel," LSWT 445, Dallas, Texas, Sept. 1974.

## *From the AIAA Progress in Astronautics and Aeronautics Series . . .*

### SCIENTIFIC INVESTIGATIONS ON THE SKYLAB SATELLITE—v. 48

*Edited by Marion I. Kent and Ernst Stuhlinger, NASA George C. Marshall Space Flight Center;  
Shi-Tsan Wu, The University of Alabama.*

The results of the scientific investigations of the Skylab satellite will be studied for years to come by physical scientists, by astrophysicists, and by engineers interested in this new frontier of technology.

Skylab was the first such experimental laboratory. It was the first testing ground for the kind of programs that the Space Shuttle will soon bring. Skylab ended its useful career in 1974, but not before it had served to make possible a broad range of outer-space researches and engineering studies. The papers published in this new volume represent much of what was accomplished on Skylab. They will provide the stimulus for many future programs to be conducted by means of the Space Shuttle, which will be able eventually to ferry experimenters and laboratory apparatus into near and far orbits on a routine basis.

The papers in this volume also describe work done in solar physics; in observations of comets, stars, and Earth's airglow; and in direct observations of planet Earth. They also describe some initial attempts to develop novel processes and novel materials, a field of work that is being called space processing or space manufacturing.

*552 pp., 6x9, illus., plus 8 pages of color plates, \$19.00 Mem. \$45.00 List*

TO ORDER WRITE: Publications Dept., AIAA, 1290 Avenue of the Americas, New York, N. Y. 10019